

Simulation App for Square-Ring Solar Absorbers Based on Metasurfaces

Borui Zhang

*School of Electronics and Information Engineering, Tiangong University, Tianjin, China
zhangborui0308@163.com*

Abstract. For efficient utilization of solar spectrum energy within 300-2500 nm, we propose a broadband solar absorber based on a metasurface with square-hollow configuration. The trilayer design employs "metal substrate/SiO₂ dielectric layer/hollow metal structure". Using COMSOL simulations, we investigate the regulatory mechanisms of material and geometric parameters on absorption performance. When zirconium (Zr) serves as the functional metal layer, the average absorption achieves 85% across 300-2500 nm, with peak efficiency approaching 100% at 1500 nm in the near-infrared regime. A COMSOL App is co-developed to democratize access, enabling cross-disciplinary intuitive control of geometric parameters. This explicitly validates Zr's broadband superiority from low-loss plasmonic resonance. The design accommodates fabrication processes including electron-beam lithography, providing an innovative pathway for solar power generation and photothermal conversion applications.

Keywords: Solar Absorber, Metasurface, COMSOL Simulation

1. Introduction

Metasurfaces utilize precisely designed subwavelength structures to effectively control light-matter interactions across multiple electromagnetic wavelengths [1]. Their unique structure-mediated light coupling mechanism offers a novel approach that not only overcomes the efficiency constraints of traditional solar absorbers but also significantly broadens their operational bandwidth [2].

While current approaches persistently explore theoretical designs to optimize solar absorption efficiency, they appear to be plagued by what seems to be universal challenges, including fabrication complexity and what tends to point toward what appears to be constrained absorption bandwidth [3]. Conventional metal-dielectric-metal structures rely on precious metals (e.g., Au, Ag) for optical field confinement, which not only ostensibly elevates fabrication costs due to material expenses but also appears to suffer from what might be characterized as narrowband resonance characteristics [4]. What seems especially noteworthy in this analytical context is that these limitations tend to impede broadband absorption performance and seemingly constrain practical implementation^[5].

Although low-cost materials like titanium (Ti) and silicon dioxide (SiO₂) are increasingly considered for metasurface absorbers due to what appears to represent their plasmonic properties, chemical stability, and abundance [6], what the evidence appears to reveal is that the absence of simulation tools enabling "low-expertise parametric control" appears to create cross-disciplinary

collaboration barriers [7]. What this pattern seems to suggest, therefore, is an impediment for non-optical specialists from participating in structural optimization, which appears to ultimately hinder the deployment of broadband absorbers [8]. Within this broader analytical framework, given the complexity of these theoretical relationships, our study focuses on what seems to constitute a metasurface-based solar absorber featuring a square-aperture configuration. What the investigation appears to indicate is that we implement a trilayer architecture comprising a metal substrate, SiO_2 dielectric spacer, and functional metal layer. Through an App with simulation capabilities, what these findings seem to point toward is that parametric manipulation of periodicity, dimensions, and material properties can be largely achieved.

2. Model structure design and result analysis

2.1. Model structure design

The proposed square metasurface solar absorber incorporates a periodic square-aperture array. As illustrated in Figure 1, each unit cell comprises three vertically stacked layers: (1) a 200-nm-thick metallic substrate (h_1), (2) a 100-nm SiO_2 dielectric spacer (h_2), and (3) a 200-nm apertured metallic top layer (h_3). This trilayer metal-dielectric-metal architecture exhibits 400 nm periodicity (P), with surface geometry featuring concentric squares - an outer 350 nm square (a) surrounding an inner 300 nm apertured square (b).

Numerical simulations were performed in COMSOL Multiphysics®. What appears particularly significant about these findings is that periodic boundary conditions were applied laterally to match what seems to constitute the structural periodicity, while perfectly matched layers (PML) were implemented along the z-direction to apparently eliminate spurious scattering at computational boundaries. Throughout simulations, what might be characterized as an air ambient was assumed. Reflection spectra were acquired via what appears to represent a 2D frequency-domain power monitor parallel to the xy-plane. Given the complexity of these theoretical relationships, the high reflectivity and optimized thickness of the bottom metallic substrate appears to tend to suggest that incident light was largely blocked with what seems to be near-zero transmittance ($T \approx 0$). What appears to follow from this analysis, absorption efficiency (A) was calculated as $A=1-R$, where R denotes reflectance.

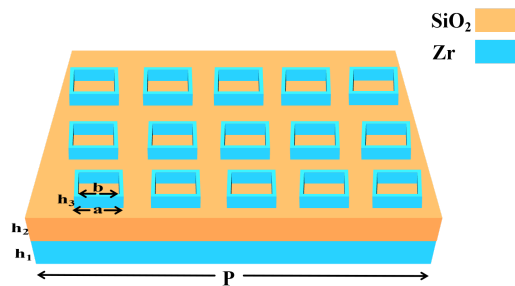


Figure 1. Schematic diagram of the metasurface

2.2. Result analysis

The absorption spectrum of the proposed metasurface-based square-architecture solar absorber, simulated via different methods in COMSOL Multiphysics®, appears to be presented in what seems to be Figure 2. What the graphical representation tends to indicate is an abscissa that apparently

spans 300-2500 nm, which seems to cover what might be characterized as the critical solar spectral region, while the ordinate appears to quantify what could be considered absorption efficiency.

Statistical analysis confirms that the Zr-based absorber achieves an average absorption efficiency of 85% across the 300-2500 nm spectrum, with its high-absorption band ($>80\%$) spanning over 1500 nm within the 500-2000 nm range. This validates its potential as a broadband solar absorber.

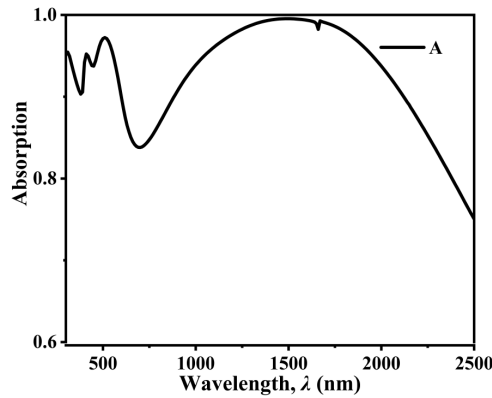


Figure 2. Average absorption rate of the metasurface

To elucidate the high-efficiency absorption mechanisms of the Zr-based absorber, electric field distributions were simulated in the xy-plane under normal illumination at key resonant wavelengths (800 nm, 1500 nm, 2300 nm). These analyses reveal light-matter interplay within the "metallic substrate/SiO₂ dielectric spacer/slotted-square metallic meta-atoms" architecture.

At an incident wavelength of 800 nm: The electric field distribution (Fig. 3a) appears to suggest what seems to be a strong field enhancement predominantly localized at the edges of the perforated square metallic resonators and at the interface between the SiO₂ dielectric layer and the metal film, which tends to point toward what appears to be a substantial contribution from Localized Surface Plasmon Resonance (LSPR) [9]. What the data seems to suggest is that regions of high field intensity are ostensibly distributed along the perimeter of the square resonators, which appears to indicate what might be characterized as the excitation of Localized Surface Plasmon Resonance (LSPR) [10]. Within this broader analytical framework, the free electrons in the metal are apparently driven by the optical field at the structural edges, leading to what seems to constitute collective oscillations that appear to convert optical energy into Joule heating via ohmic losses [11]. What appears particularly significant about these findings is that, considering the nuanced nature of these interactions, the electric field extends into the SiO₂ dielectric layer, seemingly enhancing light-matter interactions and what tends to emerge as theoretically important [12] - a synergistic improvement in the absorption efficiency in the shorter-wavelength range.

At an incident wavelength of 1500 nm: the electric field profile (Fig. 3b) reveals two distinct enhancement regions: (1) a central hotspot generated by Fabry-Pérot resonance in the metal-dielectric-metal cavity, where constructive interference of multiply reflected waves creates standing wave patterns that intensify light-matter interaction [13]. (2) perimeter confinement resulting from localized surface plasmon resonance excitation. This dual-resonance coupling synergistically achieves near-unity absorption ($\approx 100\%$), representing the dominant mechanism for broadband performance enhancement.

At an incident wavelength of 2500 nm: The electric field distribution (Fig. 3c) appears to suggest what seems to be strong field confinement within the SiO₂ dielectric layer and at the interfaces between the metallic structures and the substrate. What this phenomenon tends to indicate, within

this broader analytical framework, is what might be characterized as Propagating Surface Plasmon Resonance (PSPR) [14], where the optical field apparently propagates along the metal-dielectric interfaces, seemingly exciting collective oscillations of free electrons [15]. What appears particularly significant about these findings is that the periodic arrangement of the perforated square resonators seems to couple efficiently with the long-wavelength incident light. Given the complexity of these theoretical relationships, what the evidence appears to reveal is a synergistic interaction that appears to substantially extend the optical propagation path within the structure, thereby ostensibly maintaining high absorption efficiency ($>70\%$) in the majority of cases in the long-wavelength regime and what seems to represent an effective compensation for what appears to be the inherent limitation of single-element structures in absorbing long wavelengths.

The analysis of electromagnetic field distributions and spectral response indicates that the Zr-based metasurface absorber achieves high-efficiency broadband absorption through the synergistic effects of Localized Surface Plasmon Resonance (LSPR), Propagating Surface Plasmon Resonance (PSPR), and Fabry-Pérot (FP) cavity resonance. In the short-wavelength regime (300–1000 nm), LSPR dominates, with enhanced local fields at resonator edges strengthening light-matter interactions and enabling efficient visible-light trapping [16]. The mid-wavelength range (1000–2000 nm) exhibits a combined LSPR-FP resonance mechanism, where standing waves at resonator centers enhance ohmic losses while perimeter-localized LSPR fields broaden absorption bandwidth, ensuring strong near-infrared performance [17,18]. At longer wavelengths (2000–2500 nm), PSPR couples with lattice-induced mode confinement, leveraging propagation characteristics to sustain high mid-infrared absorption. This multi-resonance strategy overcomes the bandwidth limitations of single-mode systems, enabling efficient absorption across 300–2500 nm.

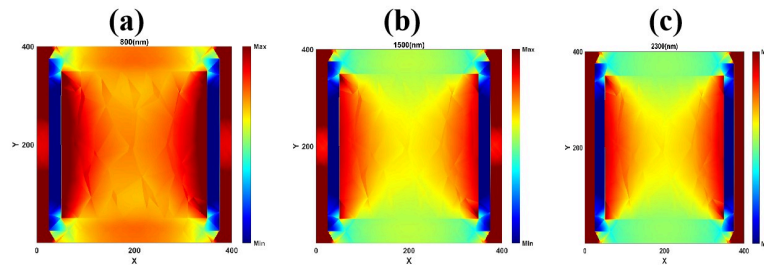


Figure 3. Electric field distribution

Figure 4 reveals that zirconium (Zr) exhibits superior broadband absorption characteristics: sustaining $>80\%$ efficiency across 500–2000 nm with a peak approaching 100% near 1500 nm wavelength, enabling efficient near-infrared energy harvesting. Although absorption progressively declines to $>70\%$ within 2000–2500 nm, it maintains effective coverage over the primary energy region of the solar spectrum. In contrast, chromium (Cr) maintains relatively stable absorption ($\approx 80\text{--}90\%$) across the spectrum but exhibits weaker peak intensity than Zr with pronounced attenuation beyond 1500 nm. Titanium nitride (TiN) sustains high absorption only transiently within the visible regime, decaying rapidly above 1000 nm, demonstrating the lowest broadband compatibility among the three materials.

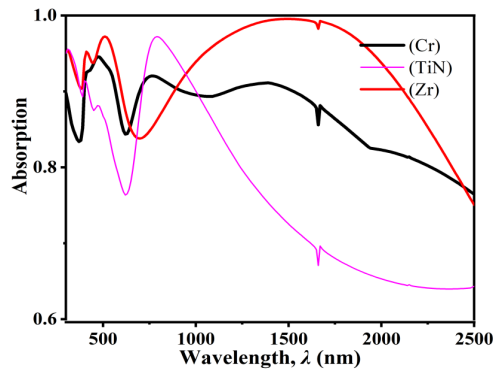


Figure 4. Comparison of absorption rates of different materials

3. App design

3.1. Comsol-based multiphysics simulation application development

Leveraging the COMSOL Multiphysics® simulation platform, this work appears to develop what seems to be a custom simulation application that tends to integrate its Wave Optics Module with core electromagnetic solvers. What this implementation appears to suggest is the potential for both reconstruction of what might be characterized as structure-electromagnetic coupling behavior in metasurface-based square absorbers and what seems to constitute cross-disciplinary analysis capabilities [19].

3.2. Comsol-enabled precision model encapsulation

Within this broader analytical framework of the COMSOL Multiphysics® environment, a three-dimensional multilayer metasurface structural model was constructed. What seems especially noteworthy in this analytical context is that, utilizing the Electromagnetic Waves, Frequency Domain physics interface, periodic boundary conditions, Perfectly Matched Layers (PML), and broadband plane wave incidence were apparently configured. Furthermore, what the evidence appears to reveal is that the dielectric constants of metals (Zr, Cr, TiN) and the optical parameters of SiO₂ were predominantly imported from the material library. What this pattern seems to suggest, therefore, is the potential for comprehensive replication of the coupled multi-mechanism behavior involving what appears to represent Localized Surface Plasmon Resonance (LSPR), Fabry-Pérot (FP) cavity resonance, and Propagating Surface Plasmon Polariton Resonance (SPPR) [20].

3.3. Barrier-free interaction design logic

Leveraging the COMSOL App Builder, what appears to be a specialized simulation workflow was encapsulated into what seems to constitute a standalone application. The core design philosophy tends to suggest what appears to be an emphasis on balancing accessibility with high-fidelity computation. What seems particularly significant about these findings, within this broader analytical framework, is that during user-defined parameter adjustments, the backend apparently automatically invokes COMSOL's parametric sweep and real-time solving modules. What this appears to suggest, therefore, is the elimination of what might be characterized as a need for custom simulation scripting or manual reconfiguration of physical field boundaries in the majority of cases.

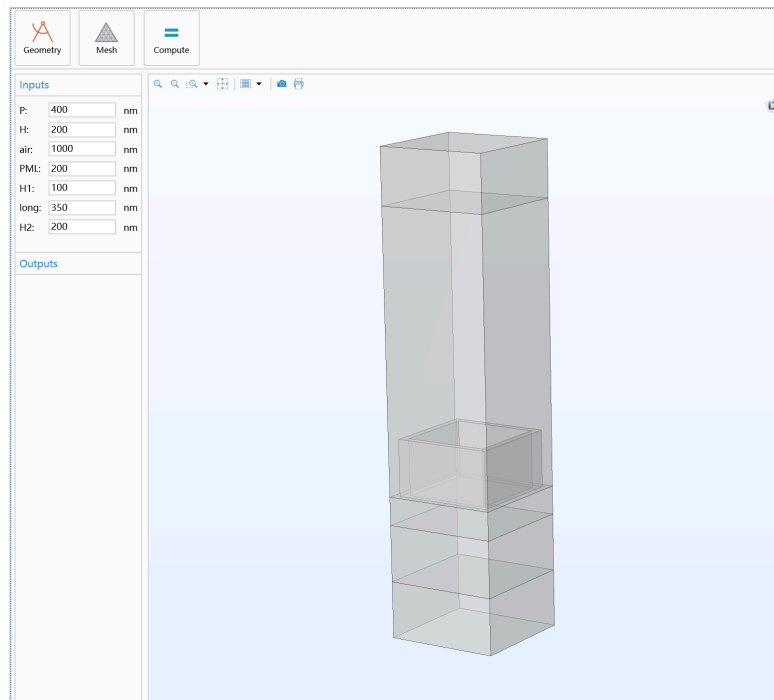


Figure 5. APP interface

4. Conclusion

This study demonstrates a broadband metasurface solar absorber featuring a square-apertured trilayer architecture (metal/SiO₂/metal). Utilizing zirconium (Zr) as the functional layer, the device exhibits 85% average absorption across the solar spectrum with near-unity peak efficiency ($\approx 100\%$) at 1500 nm. The proposed design establishes a new paradigm for high-efficiency solar energy harvesting and photothermal conversion, while advancing the development of next-generation broadband absorption devices through its innovative structural approach

References

- [1] Shen F , Chen G , Lin M , et al.Design and performance study of a full-bandwidth mid-wave infrared metasurface absorber based on deep learning optimization [J].Optics Communications, 2025, 591132171-132171.
- [2] Zhao J , Meng Z .High-Sensitivity Refractive Index Sensing Based on a Dual Ultra-narrowband Terahertz Metasurface Absorber [J].Plasmonics, 2025, (prepublish): 1-12.
- [3] Das D , Samal R R , Dikshit P A , et al.Wideband Microwave Absorption-Dominant EMI Shielding Using Metasurface-Based Absorber with Barium Titanate Ceramic Substrate for X-Band and Ku-Band Application [J].Journal of Electronic Materials, 2025, (prepublish): 1-23.
- [4] Lu C , Chen Y , Shi J , et al.Inverse design of tubular energy absorbers formed from the least-symmetric crystallographic DDC surface [J].International Journal of Solids and Structures, 2025, 320113508-113508.
- [5] Wang H , Han Q , Lv H .Structural design of low-frequency broadband adaptive nonlinear underwater acoustic absorption metasurface [J].Applied Acoustics, 2025, 240110894-110894.
- [6] Ahmed S , Alam T , Soliman M M , et al.Enhanced structural tunability and high sensitivity of a THz metasurface absorber for precise automotive fuel characterization [J].Scientific Reports, 2025, 15(1): 22996-22996.
- [7] Wang L , Li H , Shen X , et al.Transparent metasurface absorber with wide-angle stability via gradient AgNWs/PDMS heterostructure. [J].Optics letters, 2025, 50(13): 4414-4417.
- [8] Armghan A , Aliqab K , Alsharari M .A novel fan-shaped ultrabroadband solar absorber using nickel-based plasmonic metasurfaces [J].Scientific Reports, 2025, 15(1): 21839-21839.

- [9] Chen D , Takahara J .Enhancement of excitonic absorption in WS₂ mediated by Huygens Si metasurfaces. [J].Optics letters, 2025, 50(13): 4246-4249.
- [10] Wen Y , Zhu H , Song F , et al.Surface-enhanced infrared absorption (SEIRA) based on Metasurface: Principles, biochemical sensing applications, and future perspective. [J].Spectrochimica acta. Part A, Molecular and biomolecular spectroscopy, 2025, 344(Pt 1): 126621.
- [11] Lv T , Yu B , Wang Y , et al.Broadband terahertz metasurface incorporating vanadium dioxide: Achieving switchable absorber to half-wave plate and directional quarter-wave plate [J].Optics Communications, 2025, 590132013-132013.
- [12] Li D J , Lv Y , Wang H Y , et al.VO₂-integrated multifunctional terahertz metasurface: From polarization converter to absorber [J].Physics Letters A, 2025, 553130695-130695.
- [13] Fu C , Wang X , Zhu Y , et al.A Multifunctional Terahertz Metasurface with Absorption and Polarization Conversion Based on Vanadium Dioxide and Photoconductive Silicon [J].Plasmonics, 2025, (prepublish): 1-17.
- [14] Tekşen A F , Altıntaş O , Çolak B , et al.Ultrawideband Lu chaotic surface-based microwave absorber design for stealth applications [J].Journal of Computational Electronics, 2025, 24(4): 112-112.
- [15] Akhtar N M , Basha B , Younas M , et al.Absorptivity and magnetodielectric evaluations of rare earths (Gd³⁺, Pr³⁺, Ho³⁺) and transition element (Bi³⁺) doped Cd-Ni-Zn ferrite meta surface absorbers: Modeling and simulations [J].Surfaces and Interfaces, 2025, 68106698-106698.
- [16] Grayli V S , Patel T , Kasteren V B , et al.Near-Unity Absorption in Semiconductor Metasurfaces Using Kerker Interference. [J].Nano letters, 2025.
- [17] Lan C , Gao Y , Gao Z , et al.Broadband Optically Transparent Absorber and Multi-Band Stealth Based on Organic Metasurface [J].Chinese Physics Letters, 2025, 42(5): 056303-056303.
- [18] Valagiannopoulos C .Causality Implications for Absorption by EM Metasurfaces [J].Nanomaterials, 2025, 15(11): 793-793.
- [19] Kumar A N , Devi R B , Bhimaavarapu K .Graphene-Infused Terahertz Metasurfaces for High-Sensitivity Refractive Index Sensing with Dual-Peak Absorption [J].Plasmonics, 2025, (prepublish): 1-16.
- [20] Fortman G D N , Krause M G , Schall P , et al.Absorption and amplification singularities in metasurface etalons with gain [J].Nanophotonics, 2025, 14(13): 2317-2329.